Light harvesting improvement of organic solar cells with self-enhanced active layer designs

Luzhou Chen, Wei E.I. Sha, and Wallace C.H. Choy*

Department of Electrical and Electronic Engineering, the University of Hong Kong, Pokfulam Road, Hong Kong, China

* *chchoy@eee.hku.hk*

Abstract: We present designs of organic solar cells (OSCs) incorporating periodically arranged gradient type active layer. The designs can enhance light harvesting with patterned organic materials themselves (i.e. self-enhanced active layer design) to avoid degrading electrical performances of OSCs in contrast to introducing inorganic concentrators into OSC active layers such as silicon and metallic nanostructures. Geometry of the OSC is fully optimized by rigorously solving Maxwell's equations with fast and efficient scattering matrix method. Optical absorption is accessed by a volume integral of the active layer excluding the metallic absorption. Our numerical results show that the OSC with a self-enhanced active layer, compared with the conventional planar active layer configuration, has broadband and wide-angle range absorption enhancement due to better geometric impedance matching and prolonged optical path. This work provides a theoretical foundation and engineering reference for high performance OSC designs.

OCIS codes: (350.6050) Solar energy; (230.5298) Photonic crystals.

References and links

1. E. Yablonovitch and G. Cody, "Intensity enhancement in textured optical sheets for solar cells," IEEE Trans. Electron. Dev. **29**(2), 300–305 (1982).
2. E. Yablonovitch, "Statistical ray optics," J. Opt. Soc. Am. **72**(7), 899–907 (1982).
3. S. B. Rim, S. Zhao, S. R. Scully, M. D. McGehee, and P. Peumans, "An effective light trapping configuration for thin-film for solar cells," Appl. Phys. Lett. **91**(24), 243501 (2007).
4. W. Cao, J. D. Myers, Y. Zheng, W. T. Hammond, E. Wrzesniewski, and J. Xue, "Enhancing light harvesting in organic solar cells with pyramidal rear reflectors," Appl. Phys. Lett. **99**(2), 023306 (2011).
5. J. Liu, M. A. G. Namboothiry, and D. L. Carroll, "Fiber-based architectures for organic photovoltaics," Appl. Phys. Lett. **90**(6), 063501 (2007).
6. P. Bermel, C. Luo, L. Zeng, L. C. Kimerling, and J. D. Joannopoulos, "Improving thin-film crystalline silicon solar cell efficiencies with photonic crystals," Opt. Express **15**(25), 16986–17000 (2007).
7. D. Zhou and R. Biswas, "Photonic crystal enhanced light-trapping in thin film solar cells," J. Appl. Phys. **103**(9), 093102 (2008).
8. S. B. Mallick, M. Agrawal, and P. Peumans, "Optimal light trapping in ultra-thin photonic crystal crystalline silicon solar cells," Opt. Express **18**(6), 5691–5706 (2010).
9. Y. Park, E. Drouard, O. El Daif, X. Letartre, P. Viktorovitch, A. Fave, A. Kaminski, M. Lemiti, and C. Seassal, "Absorption enhancement using photonic crystals for silicon thin film solar cells," Opt. Express **17**(16), 14312–14321 (2009).
10. D. Duché, L. Escoubas, J. J. Simon, P. Torchio, W. Vervisch, and F. Flory, "Slow Bloch modes for enhancing the absorption of light in thin films for photovoltaic cells," Appl. Phys. Lett. **92**(19), 193310 (2008).
11. A. Mihi and H. Míguez, "Origin of light-harvesting enhancement in colloidal-photonic-crystal-based dye-sensitized solar cells," J. Phys. Chem. B **109**(33), 15968–15976 (2005).
12. J. R. Tumbleston, D. H. Ko, E. T. Samulski, and R. Lopez, "Absorption and quasiguided mode analysis of organic solar cells with photonic crystal photoactive layers," Opt. Express **17**(9), 7670–7681 (2009).
13. D. H. Ko, J. R. Tumbleston, L. Zhang, S. Williams, J. M. DeSimone, R. Lopez, and E. T. Samulski, "Photonic crystal geometry for organic solar cells," Nano Lett. **9**(7), 2742–2746 (2009).
14. A. Chutinan, N. P. Kherani, and S. Zukotynski, "High-efficiency photonic crystal solar cell architecture," Opt. Express **17**(11), 8871–8878 (2009).

#162481 - $15.00 USD Received 2 Feb 2012; revised 16 Mar 2012; accepted 16 Mar 2012; published 23 Mar 2012

15. R. Biswas and C. Xu, "Nano-crystalline silicon solar cell architecture with absorption at the classical $4n^2$ limit," Opt. Express **19**(S4 Suppl 4), A664–A672 (2011).
16. W. Zhou, M. Tao, L. Chen, and H. Yang, "Microstructured surface design for omnidirectional antireflection coatings on solar cells," J. Appl. Phys. **102**(10), 103105 (2007).
17. J. D. Joannopoulos, S. G. Johnson, J. N. Winn, and R. D. Meade, *Photonic Crystals: Molding the Flow of Light,* 2nd ed. (*Princeton University Press,* Princeton, *2008).*
18. X. He, F. Gao, G. Tu, D. Hasko, S. Hüttner, U. Steiner, N. C. Greenham, R. H. Friend, and W. T. S. Huck, "Formation of nanopatterned polymer blends in photovoltaic devices," Nano Lett. **10**(4), 1302–1307 (2010).
19. D. Cheyns, K. Vasseur, C. Rolin, J. Genoe, J. Poortmans, and P. Heremans, "Nanoimprinted semiconducting polymer films with 50 nm features and their application to organic heterojunction solar cells," Nanotechnology **19**(42), 424016 (2008).
20. D. D. S. Fung, L. Qiao, W. C. H. Choy, C. Wang, W. E. I. Sha, F. Xie, and S. He, "Optical and electrical properties of efficiency enhanced polymer solar cells with Au nanoparticles in PEDOT-PSS Layer," J. Mater. Chem., doi:10.1039/c1jm12820e.
21. X. W. Chen, W. C. H. Choy, S. He, and P. C. Chui, "Comprehensive analysis and optimal design of top-emitting organic light-emitting devices," J. Appl. Phys. **101**, 113107 (2007).
22. E. D. Palik, *Handbook of Optical Constants of Solids* (Academic Press, New York, 1998).
23. A. D. Rakic, A. B. Djurisic, J. M. Elazar, and M. L. Majewski, "Optical properties of metallic films for vertical-cavity optoelectronic devices," Appl. Opt. **37**(22), 5271–5283 (1998).
24. D. M. Whittaker and I. S. Culshaw, "Scattering-matrix treatment of patterned multiplayer photonic structures," Phys. Rev. B **60**(4), 2610–2618 (1999).
25. S. G. Tikhodeev, A. L. Yablonskii, E. A. Muljarov, N. A. Gippius, and T. Ishihara, "Quasiguided modes and optical properties of photonic crystal slabs," Phys. Rev. B **66**(4), 045102 (2002).
26. A. Taflove and S. C. Hagness*, Computational Electrodynamics: The Finite-Difference Time-Domain Method,* 3rd ed. (Artech House Publishers, Boston, 2005).
27. G. Li, V. Shrotriys, J. Huang, Y. Yao, T. Moriarty, K. Emery, and Y. Yang, "High-efficiency solution processable polymer photovoltaic cells by self-organization of polymer blends," Nat. Mater. **4**(11), 864–868 (2005).
28. C. D. Wang and W. C. H. Choy, "Efficient hole collection by introducing ultra-thin UV-ozone treated Au in polymer solar cells," Sol. Energy Mater. Sol. Cells **95**, 904–908 (2011).
29. S. Bavel, E. Sourty, G. With, K. Frolic, and J. Loos, "Relation between photoactive layer thickness, 3D morphology, and device performance in P3HT/PCBM bulk-heterojunction solar cells," Macromolecules **42**(19), 7396–7403 (2009).
30. M. Born and E. Wolf, *Principles of Optics* (Pergamon Press, London, 1970).
31. J. Nelson, *The Physics of Solar Cells* (Imperial College Press, London, 2003).
32. D. Poitras and J. A. Dobrowolski, "Toward perfect antireflection coatings. 2. Theory," Appl. Opt. **43**(6), 1286–1295 (2004).

1. Introduction

Recently, thin-film organic solar cells (OSCs) have gained intensively interests for the next generation of solar cells. However, thickness of the active layer in OSCs is typically a few hundred nanometers or less due to their short diffusion length of exciton, which sets a fundamental limitation on light absorption. Consequently, improvement in light trapping is very important for their practical utilization in photovoltaics. Generally, physical guideline of light trapping involves two main approaches: geometric optics methods [1–5] and wave optics methods [6–16]. The former aims at elongating optical path inside the photoactive layer and thus enhancing photon absorption. For organic thin film solar cells with typical active layer thickness of 100nm-200nm, which is in subwavelength scale, we cannot investigate light harvesting mechanism simply by the geometric optics methods and instead wave optics properties should be considered. Photonic crystal (PC) [17], due to its strong modification of electromagnetic distribution, has attracted lots of attention and can be used to increase solar cell efficiency based on different physics mechanisms. For example, based on prolonging optical path length by diffraction, grating structure backreflector (1-D PC) [6], periodic arranged cylinders backreflector (2-D PC) [6–8] and periodic arranged spheres backreflector (3-D PC) [6] have been proposed. Distributed Bragg reflector (1-D PC), owing to its photonic band gaps (PBGs) where the propagating modes are completely forbidden, can perform 100% omni-directional reflection and thus strongly reduce the transmission loss [6,7]. Slow Bloch modes in flat photonic band structure have been studied in silicon solar cells [9], OSCs [10] and dye-sensitized solar cells [11] to extend dwell time of light in the active layer.

#162481 - $15.00 USD Received 2 Feb 2012; revised 16 Mar 2012; accepted 16 Mar 2012; published 23 Mar 2012

However, it is noteworthy that enhancement mechanisms based on PC properties require large refractive index contrast between the nanostructure and the background medium. This is achievable for inorganic solar cells but it is challenge for OSCs because all the organic materials have similar value of refractive index. Motivated by this issue, we explore new absorption improvement methods special for organic materials. Recently, OSCs with a PC active layer have been studied theoretically [10,12] and experimentally [13]. But we notice that square column shaped or cylinder shaped photoactive layer has relatively low absorption rate due to its abrupt change of optical impedance. If gradient structure is employed, such as pyramid type or cone type, normal incident light couples adiabatically with laterally scattered light and thus higher absorption performance can be achieved [14–16]. Intrigued by this problem, we present OSC designs based on periodically arranged gradient shape active layer, which can enhance light harvesting by themselves. In comparison with employing inorganic concentrators (such as silicon, silver, and gold nanostructures) into the active layer of OSC which may degrade the electrical performances of OSCs by creating recombination centers or breaking the morphology of organic materials, the self-enhanced organic active layer can both enhance the optical absorption and facilitate carrier collections simultaneously as will be described below. In modeling we employ poly-3-hexylthiophene: [17]-phenyl-C61-butyric acid methyl ester (P3HT:PCBM) blend to show the improvement because its optical and electrical properties have been well studied. As a comparison, square column type active layer and cylinder type active layer have also been discussed. Our numerical results show that both kinds of gradient-type active layers have noticeable advantages compared with traditional planar bulk active layers. Especially, only 1/3 or less amount of P3HT:PCBM will be enough to harvest same quantity of light energy if the active layer is made as pyramid shape rather than planar configuration. These designs are believed feasible experimentally because recently nanostructure patterned OSCs have been realized by the imprint methods which not only demonstrate the feasible of the making well-aligned nanoscale patterned active layer [13,18,19] but also provide new degree of freedom on introducing optical structures into the active layer directly for further improving OSCs performance for practical photovoltaics. It is therefore desirable to have theoretical studies in the well-aligned nanostructure which can show the physics and improve the device performances simultaneously.

Regarding the theoretical model, another noteworthy contribution in our work lies at the absorption power calculation based on scattering matrix method (SMM) by rigorously solving Maxwell's equations. Different from the widely-used calculation method by *Absorption = 1-Transmission-Reflection*, our algorism can extract the net optical absorption of the active layer rather than the whole OSCs. This improvement is very important because metal absorption, which does not contribute to exciton generation, can be excluded from the result.

2. Theoretical model

The studied OSC structures comprise of Indium tin oxide (ITO) anode / Zinc oxide (ZnO) injection layer / P3HT:PCBM nanostructure active layer/ P3HT:PCBM flash layer/ Lithium fluoride (LiF) electron transport layer /aluminum (Al) cathode. Our proposed structure with periodic arranged pyramids of P3HT:PCBM blend in the ZnO background are shown in Fig. 1(a). As a comparison, we also calculate an OSC with square column type active layer. Another set of OSCs with cone type active layer and cylinder type active layer are depicted in Fig. 1(b). In modeling, we employ complex refractive index of P3HT:PCBM measured by ellipsometer [20]. In some papers, ITO and ZnO are taken to be transparent over the involved wavelength range, but in our calculation we did not make this approximation, optical parameters of ITO and ZnO are taken from Ref [21]. and Ref [22], respectively. The complex refractive index of Al is calculated based on the Brendel-Bormann model [23].

#162481 - $15.00 USD Received 2 Feb 2012; revised 16 Mar 2012; accepted 16 Mar 2012; published 23 Mar 2012

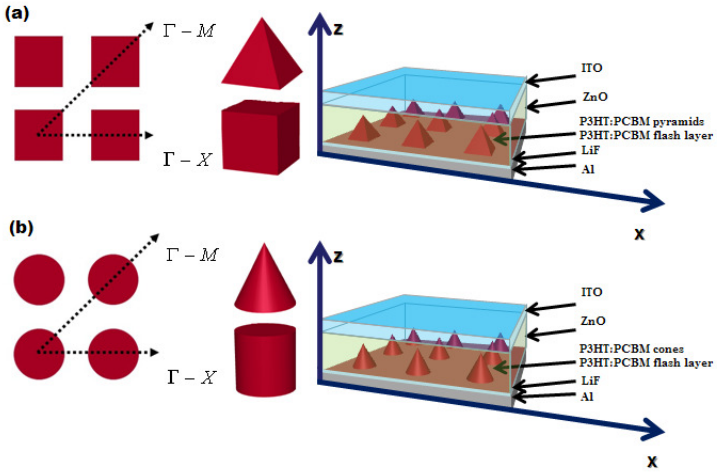

Fig. 1. Schematic illustration of (a) organic solar cell (OSC) with periodic arranged pyramids or square columns consist of P3HT:PCBM in the ZnO background. Top view of the lattice pattern is shown and high-symmetric Γ-M and Γ-X directions have been depicted. (b) OSC with periodic arranged cone type or cylinder type active layer.

In view of good convergence, fast speed and low memory consumption associated with the SMM method [24,25], it is employed here to investigate the optical properties of OSCs. SMM is a convenient algorithm for modeling multilayered system with laterally patterned nano-structure. Firstly, electromagnetic field is expanded as a series of Bloch modes (plane waves). Then, the OSC is divided into sub-layers along the z-direction and the Maxwell's equations of each layer are recast into eigenvalue equations. Finally, by using the continuous tangential boundary condition of electromagnetic field, elements of the S-matrix can be obtained by recursive equations. Along the direction of propagating light, electromagnetic field of the l^{th} layer is expressed as a superposition of forward and backward propagating waves with the complex amplitudes a_l and b_l. The scattering matrix related to two layers l and l' is given by:

$$\begin{pmatrix} a_l \\ b_{l'} \end{pmatrix} = \begin{pmatrix} S_{11}(l',l) & S_{12}(l',l) \\ S_{21}(l',l) & S_{22}(l',l) \end{pmatrix} \begin{pmatrix} a_{l'} \\ b_l \end{pmatrix}. \tag{1}$$

Transmission and reflection coefficients can be calculated by Poynting vectors based on the matrix $S_{in,out}$, which connects the substrate region (corresponding to incoming waves) to the air region (corresponding to outgoing waves). It is common to calculate the absorption of solar cells straightforwardly by *Absorption = 1-Transmission-Reflection*. However, this formula essentially gives the total absorbed energy of all the layers but not the expected absorption of the active layer for photon generation. In order to handle this problem, we calculate absorption power A by taking volume integral over the active layer:

$$A = [1 - L] \cdot E_{inc}(\omega) = \int_{V_o} n(\omega) k(\omega) \varepsilon_o \omega \left| \mathbf{E}(r,\omega) \right|^2 dV, \tag{2}$$

where E_{inc} refers to the total energy of incident light, L denotes the energy loss fraction including metallic and leaky losses, and $\mathbf{E}$ is the electric field profile at the active layer. Moreover, V_o denotes the total volume of the active layer, n and k refer to the real and the imaginary parts of complex refractive index of the active layer materials, ω is the frequency of incident light, and ε_0 is the vacuum dielectric constant. It should be noted that in order to

#162481 - $15.00 USD Received 2 Feb 2012; revised 16 Mar 2012; accepted 16 Mar 2012; published 23 Mar 2012

calculate **E** in the l^{th} layer, a_l and b_l should be calculated based on matrix elements of $S(l_{in}, l)$ and $S(l,l_{out})$:

$$a_l = \left[1 - S_{12}(l_{in},l)S_{21}(l,l_{out})\right]^{-1} \times \left[S_{11}(l_{in},l)a_0\right] \quad (3)$$

$$b_l = \left[1 - S_{21}(l,l_{out})S_{12}(l_{in},l)\right]^{-1} \times \left[S_{21}(l,l_{out})S_{11}(l_{in},l)a_0\right], \quad (4)$$

where a_0 is the amplitude of incident light. By the above treatments, absorption power of the active layer can be individually determined. Our numerical results by the SMM have been benchmarked with Finite Difference Time Domain method (FDTD) [26].

3. Result and discussion

3.1 Optimization of parameters

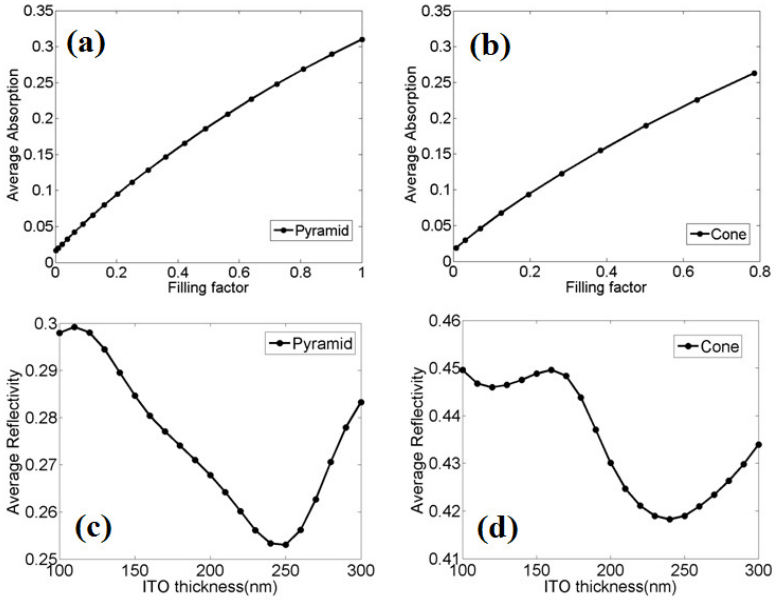

Fig. 2. (a) Average absorption as a function of filling factor $ff = s^2/a^2$ for pyramid type active layer with height h = 200nm, lattice const a = 200nm. s is the bottom side length of the pyramids. (b) Average absorption as a function of filling factor $ff = \pi R^2/a^2$ for cone type active layer with height h = 200nm, lattice const a = 200nm. R is the bottom radius of the cones. (c) Average reflectivity as a function of ITO thickness for pyramid type active layer. (d) Average reflectivity vs. ITO thickness for cone type active layer.

In modeling, although thicker active layer results in better optical absorption, it will degrade electric performance of the OSC because exciton diffusion length of P3HT:PCBM is around 10nm. Here we use typical thickness of 200 nm which have been reported by various groups in designing the device structures for practical application [27–29].The thickness of the OSC are ITO = 100nm, ZnO = 20nm, P3HT:PCBM nanostructure layer = 200nm, P3HT:PCBM flash layer = 10nm, LiF = 1nm, and Al = 100nm. These employed parameters have been optimized by experiments for achieving best device performance. Then we optimize the structure by scanning the filling factor (*ff*) with lattice const a = 200nm. For pyramid type active layer $ff = s^2/a^2$ (s is the bottom side length of the pyramid) and for cone type active layer $ff = \pi R^2/a^2$ (R is the bottom radius of the cone). Corresponding weighted average absorption is calculated by:

#162481 - $15.00 USD Received 2 Feb 2012; revised 16 Mar 2012; accepted 16 Mar 2012; published 23 Mar 2012

$$\langle A \rangle = \frac{\int_{400nm}^{800nm} A \frac{dI(\lambda)}{d\lambda} d\lambda}{\int_{400nm}^{800nm} I(\lambda) d\lambda}, \quad (5)$$

where A is absorption of the OSC and $I(\lambda)$ is the sun irradiation spectrum intensity of standard air mass 1.5(AM 1.5). We find that for both kinds of gradient type active layers, <A> increases monotonously as filling ratio increased (Figs. 2(a)-2(b)). Consequently in the following calculation we choose close packed structure for both pyramids type and cone type design.

It should be noted that some reports have detailed discussion about minimizing surface reflection by choosing ITO anode with proper thickness, which is also functioned as the anti-reflective coating (AR coating) of the solar cells. In Figs. 2(c)-2(d) we calculate average reflectivity of different ITO thickness based on a similar wavelength integral of Eq. (5). The results show that lowest reflection loss can be achieved when ITO thickness is around 240nm for both gradient type active layers. However, when we calculate the absorption power using ITO = 240nm, we found that the improvement compared with widely used 100nm is only 0.2%, consequently we still use typical 100nm thickness.

3.2 Absorption power

Obviously, besides the employed volume of P3HT:PCBM, height and lighted area also have great influence to device absorption. In order to keep a relatively fair comparison, for every pyramid or cone type OSC, we set a corresponding control planar OSC with same height and same lighted area. With this setting the planar OSC consists of three time amount of P3HT:PCBM compared to its pyramid or cone shape counterpart. Consequently, we should compare two OSCs with absorption power of per unit volume P3HT:PCBM rather than the original absorption power. Surprisingly, we found that the original absorption power of closed pack pyramid active layer is even higher than its corresponding planar control cell in 400nm-620nm wavelength range, although the later contents three times volume of P3HT:PCBM than the former(Fig. 3(a)). Unit volume absorption power of Fig. 3(a) is shown in Fig. 3(b). Average enhancement factor reaches 3.21 and maximum reaches 4.88 at 520nm. For a larger scale situation, it will reach an even higher average enhancement factor of 4.58 (Fig. 3(c)). However, as mentioned above, thick P3HT:PCBM active layer results in good optical absorption but may degrade electric performance due to low carrier mobility, and thus the power conversion efficiency will be even lower than thin OSC. Results of cone type active layer and cylinder type active layer are also shown in Fig. 3(d), indicating that cone shape performs better than cylindrical shape. It should be noted that ZnO is used as the background of all P3HT:PCBM nanostructure, while no ZnO background exists for the planar cell. Although ZnO absorption is incorporated in the results, it is too weak as compared to P3HT:PCBM absorption in λ = 400nm-800nm. Hence, we simply assume that in this wavelength range, the absorption of ZnO is zero.

#162481 - $15.00 USD Received 2 Feb 2012; revised 16 Mar 2012; accepted 16 Mar 2012; published 23 Mar 2012

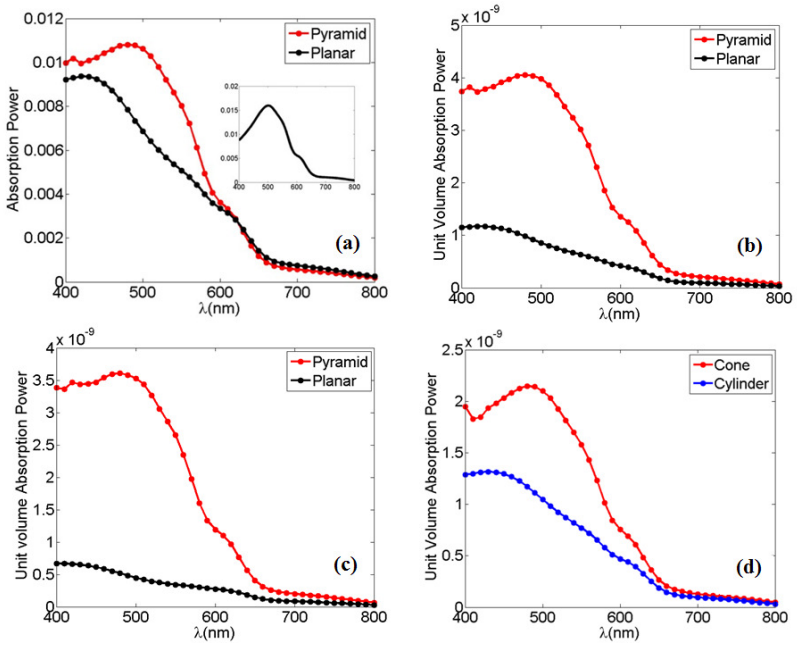

Fig. 3. (a) Absorption power of the active layer. Red line denotes the result of close packed pyramid type active layer with bottom side length s = 200nm, lattice const a = 200nm, and height h = 200nm. Black line denotes the result of planar control cell with 3 times amount of P3HT:PCBM. Its height and lighted area is equal to pyramid type OSC. The inset shows the absorption coefficient of P3HT:PCBM. (b) Absorption power of the active layer per unit volume of P3HT:PCBM. All parameters are same with (a). (c) Result of larger scale pyramid type active layer (s = 400nm, a = 400nm, h = 400nm) and corresponding planar control cell. (d)Result of closed packed cone type active layer (bottom radius R = 100nm, a = 200nm, h = 200nm) and cylinder type active layer (radius R = 100nm, a = 200nm, h = 200nm).

For our OSCs design, the transmission loss is neglectable because light transmission rate through the Al backreflector is very low, hence main energy loss of the OSC comes from reflection. That means given same quantity of incident energy, devices with lower reflectivity will result in higher absorption. As widely known, single layer quarter-wavelength AR coating is only capable to reduce reflection in limited wavelength range, while multiple layers AR coating can achieve relatively wider range reduction and the best structure is the graded index AR coating (GRIN AR coating) which has broadband effect due to better impedance matching. Our OSC design with gradient active layer can offer the improvement as from the linear GRIN system. The gradient-type active layer has a linear geometric transition of refractive index from top to bottom while GRIN structure has linear continuous changed refractive index from top to bottom. By dividing these inhomogeneous systems into N sub-layers, effective refractive index of the i^{th} sub-layer can be calculated approximately:

$$n_i = ff_i \cdot n_A + (1 - ff_i) \cdot n_B, \tag{6}$$

for pyramid or cone shape situation, ff_i is the filling factor of the i^{th} sub-layer, while for GRIN system ff_i is a generalized quantity denoting the weighted refractive index. Consequently, although linear GRIN system and gradient shape system are physically different, using this effective medium approximation (EMA), they can be mathematically equivalent. That is why they both have similar broadband reflection reduction compared with planar structure. If precise study is involved, GRIN system should be simulated by more complicated model such as Bruggeman EMA [30].

#162481 - $15.00 USD Received 2 Feb 2012; revised 16 Mar 2012; accepted 16 Mar 2012; published 23 Mar 2012

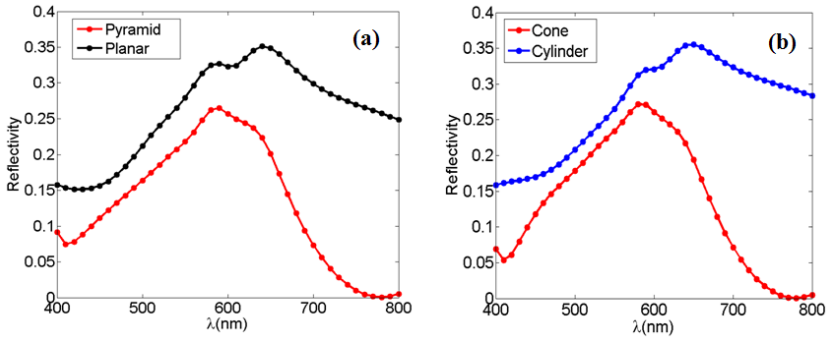

Fig. 4. (a) Reflectivity of close packed pyramid type active layer (red line) and planar active layer (black line). (b) Reflectivity of cone type active layer (red line) and cylinder type active layer (blue line).

To verify our declaration, we calculate reflectivity of the active layer as Fig. 4 shown. Since spacer and electrode layers will affect the optical environment of the multilayered OSC structure, here we simplify the structure to be a bare patterned active layer. According to Fig. 4, since reflectivity also equals to $(Z_{blend}-Z_{air})/(Z_{blend}+Z_{air})$ (where Z_{blend} and Z_{air} are optical impedance of P3HT:PCBM blend and air, respectively), we can see that gradient shape active layer reflects less energy than column shape active layer due to better impedance matching. In comparison with the abrupt change in the column or planar case, better coupling can be expected between the incident light and the laterally scattered light. It should be noted that fabrication of GRIN system is a challenging work because choosing proper material and precise control of the inhomogeneous refractive index profile is rather difficult. So it is very challenging to fabricate a GRIN active layer for broadband absorption enhancement, especially for organic materials. Our structures offer possible designs which have same advantage of linear GRIN system on reducing device reflection loss and thus enhancing light absorption.

Another reason of the absorption improvement is that light in the periodic patterned nanostructure has longer optical path and longer dwell time due to multiple scatters, which can compensate for the reduced OSC thickness. According to the Beer-Lambert's law, the absorption length of photon, although depends on materials, generally has an increasing trend as wavelength increases. Firstly, this law can explain the absorption power shown in Fig. 3, which is similar with the P3HT:PCBM absorption coefficient (inset of Fig. 3(a)), but in short wavelength range the absorption is obviously enhanced. It is because photon in shorter wavelength range does not require long optical path and thus has priority of being absorbed compared with longer wavelength photon. Secondly, the law suggests that to absorb photons in longer wavelength regions, the corresponding planar active layer should be made thicker. PC structure can diffract light efficiently and thus light can traverse through the active layer for multiple times, leading to efficient absorption. Such kind of mechanism, which contributes to prolonging optical path length, has a similar effect of the situation that light propagates through a very thick planar photoactive layer. As a result, periodic nano-structures are quite suitable for photon absorption in long wavelength. Especially, pyramid has been proved to be the most efficient scatterer compared to other shapes due to its low degree of symmetry, which has similar light trapping performance as ideal Lambertian surface [31].

#162481 - $15.00 USD Received 2 Feb 2012; revised 16 Mar 2012; accepted 16 Mar 2012; published 23 Mar 2012

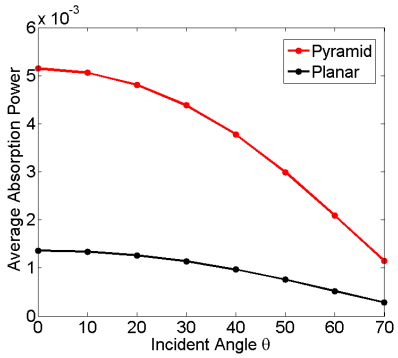

Fig. 5. Average absorption power of the active layer as a function of the incident angle θ: (red line) the closed packed pyramid type OSC with a = 200nm, s = 200nm and h = 200nm; (black line) corresponding planar bulk control solar cell using same volume of P3HT:PCBM and same active layer thickness.

We also investigate the average absorption power with incident angle θ as shown in Fig. 5. The result shows that over a wide angular range, our gradient type active layer has better absorption than planar OSC with same volume of P3HT:PCBM. This is very important for OSC application because the incident angle of sunlight always changes dynamically. It is worth point out that although linear GRIN structure has similar optical property of gradient shape structure as discussed above, it cannot keep good performance at large incident angle. Quintic refractive index profile has been proposed to improve oblique incident absorption but it also faces the challenge of fabrication [32].

3.3 Exciton generation

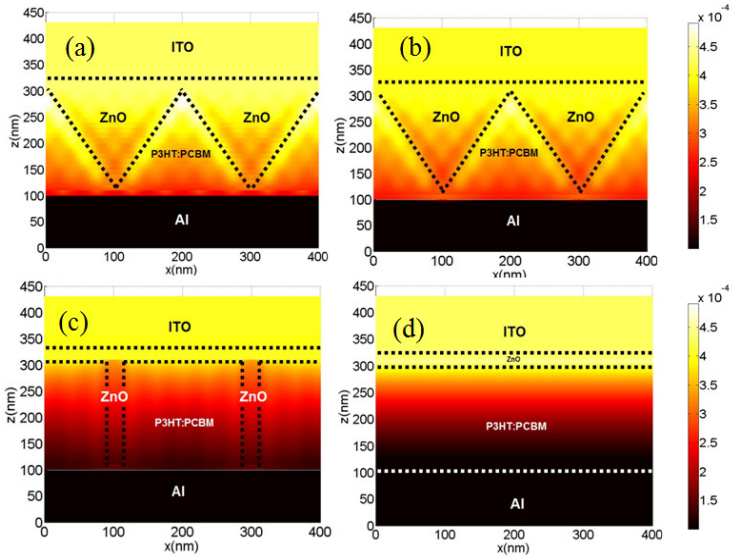

Fig. 6. Electric field profile (incident wavelength λ=500nm) of: (a) the pyramid type OSC, a=200nm, h=200nm, s=200nm (close packed); (b) the cone type OSC, a=200nm, h=200nm, R=100nm (close packed); (c) the cylinder type OSC, bottom radius R=95nm (loose packed); (d) the planar OSC. All figures are drawn with the same color scale.

Electric field profiles of OSC with pyramid type active layer and cone type active layer under incident wavelength λ=500nm are shown in Fig. 6(a) and 6(b) respectively. Remarkably, there is more energy penetrating into the absorption material, which is significantly different

#162481 - $15.00 USD Received 2 Feb 2012; revised 16 Mar 2012; accepted 16 Mar 2012; published 23 Mar 2012

from the cylinder case (Fig. 6(c)) and planar OSC (Fig. 6(d)) where the incident energy evanesced quickly. In other words, when same volume of P3HT:PCBM blend is employed, more light can be absorbed by gradient shape active layer.

Further, when energy (photons) is absorbed by P3HT:PCBM, excitons will be created. Assuming one incident photon can generate one exciton, we calculate the exciton generation profile in the photoactive layer by the time average dissipation energy <Q>:

$$G(r,\omega) = -\frac{\nabla \cdot \langle S \rangle}{E_0(\omega)} = \frac{\langle Q \rangle}{E_0(\omega)}, \tag{7}$$

where <S> refers to the time average Poynting vector and $E_0(\omega)$ is the energy of a single photon. Figure 7 shows exciton generation distribution at the position z=50nm of the cone shape active layer (Fig. 7(a)) and cylinder shape active layer (Fig. 7(b)). Due to deeper penetration of energy in cone type active layer, exciton creation is obviously more efficient and this predicts more efficient utilization of absorption material.

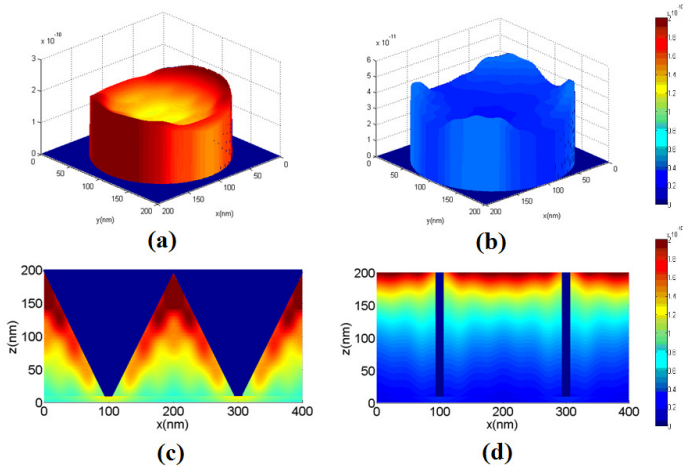

Fig. 7. (a) Exciton generation profile at z = 50nm for cone type active layer(R = 95nm). (b) Exciton generation profile at the same z position of cylinder type active layer(R = 95nm). (c)-(d) Vertical cross view of exciton generation profile of cone type and cylinder type active layer. All figures are drawn with the same color scale.

Vertical cross view of exciton generation profile of these two structures are depicted in Figs. 7(c) and 7(d). According to the figures, in cone shape active layer most of the excitons are created at the position which is near to the interface between P3HT:PCBM and ZnO. This phenomena has important meaning for device electric property because exciton diffusion length in P3HT:PCBM is only around 10nm. Shorter exciton creation distance will result in higher carrier collection rate. Pyramid type active layer also has this advantage so here we did not show those similar results.

4. Conclusion

We theoretically study organic solar cells (OSCs) with periodically arranged gradient type active layer based on self-enhanced mechanism. The results show that these structures have broadband (400nm-800nm) and wide angle range absorption enhancement compared with conventional planar OSCs due to better geometric impedance matching and longer optical path. This work can contribute to improve the nano-patterned OSCs efficiency in practical photovoltaic applications.

#162481 - $15.00 USD Received 2 Feb 2012; revised 16 Mar 2012; accepted 16 Mar 2012; published 23 Mar 2012

Acknowledgments

This work is supported by UGC grant (#10401466) of the University of Hong Kong, the General Research Fund (HKU#712010) from the Research Grants Council of Hong Kong Special Administrative Region, China.

#162481 - $15.00 USD Received 2 Feb 2012; revised 16 Mar 2012; accepted 16 Mar 2012; published 23 Mar 2012